

The heparin-binding domain of IGFBP-2 has IGF binding-independent biologic activity in the growing skeleton

Masanobu Kawai^{1,2}, Anne C Breggia¹, Victoria E DeMambro¹, Xinchun Shen³, Ernesto Canalis⁴, Mary L Bouxsein⁵, Wesley G Beamer⁶, David R Clemmons³, Clifford J Rosen¹

From Center for Clinical and Translational Research, Maine Medical Center Research Institute, Scarborough, Maine 04074, USA¹, Department of Bone and Mineral Research, Osaka Medical Center and Research Institute for Maternal and Child Health, Izumi, Osaka 594-1101, Japan², Department of Medicine, University of North Carolina, School of Medicine, Chapel Hill, North Carolina 27599, USA³, Department of Research, Saint Francis Hospital & Medical Center, Hartford, Connecticut 06105, USA⁴, Orthopaedic Biomechanics Laboratory, Beth Israel Deaconess Medical Center and Harvard Medical School, Boston, Massachusetts 02215, USA⁵, The Jackson Laboratory, Bar Harbor, Maine 04609, USA⁶.

Running title: Heparin-binding domain of IGFBP2 is anabolic to growing bone

Address correspondence and requests for reprints to; Dr. Clifford J Rosen, Maine Medical Center Research Institute, 81 Research Drive, Scarborough, ME, 04074-7205, USA, TEL: +1-207-885-8100, FAX: +1-207-885-8174, E-mail: ROSENC@mmc.org

Insulin-like growth factor-binding 2 (IGFBP-2) is a member of a family of six highly conserved IGF binding proteins (IGFBPs) that are carriers for the IGFs. IGFBP-2 levels rise during rapid neonatal growth and at the time of peak bone acquisition. In contrast, *Igfbp2*^{-/-} mice have low bone mass accompanied by reduced osteoblast numbers, low bone formation rates, and increased PTEN expression. In the current study we postulated that IGFBP-2 increased bone mass partly through the activity of its heparin-binding domain (HBD). We synthesized a HBD-peptide specific for IGFBP-2 and demonstrated *in vitro* that it rescued the mineralization phenotype of *Igfbp2*^{-/-} bone marrow stromal cells (BMSCs) and calvarial osteoblasts (COBs). Consistent with its cellular actions, the HBD-peptide *ex vivo* stimulated metacarpal periosteal expansion. Furthermore, administration of HBD-peptide to *Igfbp2*^{-/-} mice increased osteoblast number, suppressed marrow adipogenesis, restored trabecular bone mass and reduced bone resorption. Skeletal rescue in the *Igfbp2*^{-/-} mice was characterized by reduced PTEN expression followed by enhanced Akt phosphorylation in response to IGF-I, and increased β -catenin signaling through two mechanisms: 1-stimulation of its cytosolic accumulation and 2-increased phosphorylation of serine552. We conclude that the HBD-peptide of IGFBP-2 has anabolic activity by activating IGF-I/Akt and β -catenin signaling pathways. These data support a growing body of evidence that

IGFBP-2 is not just a transport protein but rather that it functions coordinately with IGF-I to stimulate growth and skeletal acquisition.

IGF (Insulin-like growth factor) binding protein-2 (IGFBP-2) is a member of a highly conserved family of six IGFBPs which circulate or reside locally in the extracellular space including the bone marrow micro-environment (1-3). IGFBP-2 has high-affinity for IGF-I/IGF-II and is believed to regulate IGF bioavailability in the pericellular environment. IGFBP-2 is the second most abundant circulating IGFBPs and is expressed in several mammalian tissues including the skeleton (2). Growing evidence demonstrates that increased IGFBP-2 levels are associated with reduced adipose tissue mass and improved glucose metabolism both in human and mouse models (4-6). Hedbacker et al. recently reported that IGFBP-2 exhibits acute glucose-lowering properties in several diabetic mouse models and that IGFBP-2 may mediate some of leptin's metabolic activity (5). However the role of IGFBP-2 in skeletal homeostasis is less clear and is dependent on the experimental model system. Generally, IGFBP-2 has been shown to inhibit IGF-I actions *in vitro* (3). Also, over-expression of *Igfbp2* inhibits growth hormone (GH)-stimulated chondrocytic expansion in GH transgenic mice (7). However, Khosla et al. reported that IGFBP-2 markedly stimulated bone formation in patients with hepatitis C-associated osteosclerosis and the administration of IGFBP-2 + IGF-II prevented bone loss in immobilized rats (8,9). Furthermore, we recently showed that

Igfbp2^{-/-} mice had markedly impaired bone formation, reduced trabecular bone volume fraction, altered micro-architecture and low bone turnover, suggesting that IGFBP-2 might be extremely important within the skeletal milieu (10).

In addition to its IGF-I binding dependent actions, IGFBP-2 and other IGFbps have been shown to stimulate biologic responses that are independent of their abilities to bind to IGFs (3). Similarly Lodish and colleagues recently demonstrated that IGFBP-2 alone could stimulate hematopoietic stem cells *ex vivo*, although the mechanism of its action was not described (11). Previously, IGFBP-2 was reported to bind to extracellular matrices (12,13). More recently several lines of evidence show that the heparin-binding domain (HBD) plays a role in IGFBP-2 function. Russo et al. reported that IGFBP-2 was proteolytically cleaved and that smaller fragments which include HBD still possessed the capacity to bind to extracellular matrix and with low affinity to IGF-I (14). They also demonstrated that IGFBP-2 stimulated the proliferation and metastatic behavior of neuroblastoma cells through the HBD (15). Interestingly, zebrafish IGFBP-2 lacks the HBD and cannot bind to any extracellular matrix (16). Taken together, these results suggest that IGFBP-2-binding to extracellular matrix is likely to be dependent on the HBD.

PTEN (phosphatase and tensin homolog deleted on chromosome 10) is a lipid phosphatase that opposes IGF-I signaling by dephosphorylating phosphatidylinositol-3,4,5-trisphosphate (PIP3) to phosphatidylinositol-4,5-diphosphate (PIP2) (17). Mice lacking PTEN only in osteoblasts showed progressively increasing bone mass with age indicating the important role of PTEN and the PI3K (Phosphatidylinositol 3-kinase)/Akt signaling pathway in bone maintenance (18). There is also a negative correlation between IGFBP-2 and PTEN expression in certain types of tumor cells (19-21). Moreover, we reported that PTEN expression was enhanced in osteoblasts derived from *Igfbp2*^{-/-} bone marrow stromal cells (10). Interestingly, Perks et al. suggested that IGFBP-2 suppression of PTEN was mediated in an IGF binding independent manner (20). Because Akt activation is a critical factor regulating bone mass (22,23), we speculated that IGFBP-2 could enhance Akt signaling by suppressing PTEN expression independent of IGF-I binding and that

the HBD is involved in the down-regulation of PTEN.

IGFBP-2 contains two putative HBDs; one HBD in the C-terminus domain shares the sequence similarity with other HBD containing IGFbps such as IGFBP-3 and IGFBP-5 (3). On the other hand, the HBD in the linker region is unique and is not present in other IGFbps. Based on the unique sequence of the IGFBP-2 HBD subsequently referred to simply as the HBD, we generated a peptide corresponding to the one in the linker region, and tested whether the HBD peptide affected skeletal turnover. We found that the HBD peptide has an anabolic effect on the skeleton through suppression of PTEN in osteoblasts and that this effect was mediated by enhanced Akt and β -catenin signaling. Moreover, there was significant synergy between the HBD and IGF-I in respect to enhancement of pAKT and β -catenin production.

Experimental Procedures

Mice-Generation of the original mixed background strain, B6;129-*Igfbp2*<*tm1**Jep*>, which we refer to *Igfbp2*^{-/-} mice, has been described previously (10,24). The original mice were backcrossed onto C57BL/6J background for 10 generations. *Igfbp2*^{+/+} mice were C57BL/6J controls. All experimental studies were performed with male mice. All the animal studies were reviewed and approved by the Institutional Animal Care and Use Committee of Maine Medical Center Research Institute.

Cell culture-MC3T3-E1 cells were purchased from ATCC and maintained in α MEM containing 10% FCS Neonatal calvarial osteoblasts were collected from 7-10 day old mice. Briefly, calvariae were digested 5 times with collagenase P and trypsin. Cells released from digests 2 through 5 were collected as primary calvarial osteoblasts and maintained in DMEM supplemented with 10% FCS and non-essential amino acids. Osteoblastogenesis of primary calvarial osteoblasts was analyzed by treating cells with 4 mM of β -glycerophosphate and 50 μ g/ml of ascorbic acid in α MEM with 10% FCS. Bone marrow stromal cells (BMSCs) were harvested from femurs and tibias of 8 weeks old mice. BMSCs were grown in α MEM containing 10%

FCS. Osteoblastogenesis of BMSCs was induced by the treatment with osteogenic media consisting of α MEM containing 10% FCS, 8 mM β -glycerophosphate, and 50 μ g/ml ascorbic acid.

Metacarpal culture-Metacarpals were isolated from *Igfbp2*^{-/-} mice from 1-day old mice and incubated in DMEM containing 0.5% BSA, 50 μ g/ml ascorbic acid and 1 mM β -glycerol phosphate for 10 days. Stimulants were added to culture media from day 1. At day 10, metacarpals were incubated in media containing calcein (500 ng/ml) for 2 hours for staining of calcium deposition and images were obtained. Bones were then fixed with 4% PFA, embedded in paraffin, and processed for Alcian blue and von Kossa double staining.

Real-time RT-PCR-Total RNA was prepared using RNeasy Mini Kit (Qiagen). cDNA was generated using a random hexamer and reverse transcriptase (Superscript III, Invitrogen) according to the manufacturer's instructions. Quantification of mRNA expression was carried out using an iQ SYBR Green Supermix in a iQ5 thermal cycler and detection system (Bio-Rad). GAPDH was used as an internal standard control gene for all quantification. Primer sequences are available upon request.

Western blot analysis-To prepare whole cell lysates, cells were solubilized in RIPA buffer (50 mM Tris, 150 mM NaCl, 1 mM EDTA, 1% NP-40, 0.25% Na-deoxycholate, 2 μ g/ml aprotinin, 2 μ g/ml leupeptin, 2 μ g/ml pepstatinA, 0.5 mM phenylmethylsulfonyl fluoride, and 1 mM dithiothreitol). To isolate the cytosolic fraction, cells were solubilized with hypotonic buffer containing protease and phosphatase inhibitors (10 mM Tris, 0.2mM MgCl₂, pH 7.4) and kept on ice for 10 min. Cell lysates were mixed with sucrose buffer (final concentration; 25mM Sucrose, 0.1 mM EDTA) and centrifuged at 20,000 x g for 1 hour. The supernatant contained the cytosolic fraction. To prepare the membrane fraction, cells were solubilized with PBS containing protease and phosphatase inhibitors. The lysates were frozen at -80 °C for 1 h and thawed at room temperature. After three cycles, they were centrifuged at 13,000 x g for 25 min. The pellet was resuspended with membrane protein isolation buffer (20 mM Tris-HCl; 150 mM NaCl; 1 mM EDTA; 1 mM EGTA; and 1% Triton X-100, pH 7.5) containing protease and phosphatase inhibitors. Equal amounts of

sample were separated by SDS-PAGE and transferred electrophoretically to nitrocellulose membranes. Membranes were blocked in 5% BSA in Tris-buffered saline. Thereafter, the membranes were immunoblotted with anti-PTEN (Cell signaling), anti-Akt (Cell signaling) anti-pSer473-Akt (Cell signaling), anti- β -catenin (BD Transduction Laboratories, 610153), anti-pSer552- β -catenin(Cell signaling), or anti- β -actin (Santa Cruz), and developed with horseradish peroxidase-coupled anti mouse or rabbit IgG antibodies, followed by enhancement with SuperSignal West Dura Extended Duration Substrate Antibodies (Pierce Chemical Co.).

Immunoprecipitation with Akt1 and Akt2

Cells were starved with serum-free medium (SFM) overnight and then exposed to 0 or 50 ng/ml IGF-I for 10 min. The cells were lysed with RIPA buffer. The cell lysates were centrifuged at 14,000 \times g for 10 min at 4 °C. They were immunoprecipitated with either anti-Akt1 antibody(1:500) or anti-Akt2 antibody(1:500) overnight at 4 °C. The immunoprecipitates were immobilized using protein-A-Sepharose beads for 2 h at 4°C and washed three times with the same buffer. The precipitated proteins were eluted in 40 μ l of 2 \times Laemmli sample buffer, boiled for 5 min, and separated using 10 % SDS-PAGE. The proteins were then transferred to Immobilon-P membranes. The blots were incubated overnight at 4 °C with the indicated antibodies. The proteins were visualized using enhanced chemiluminescence (Pierce).

Generation of heparin-binding domain peptide

The synthetic peptide containing the heparin binding domain (AA196-199) and 9 additional amino acids of mouse IGFBP2, ¹⁸⁸KHLSLEEPKCLR²⁰⁰ (referred to as HBD-peptide), and control peptide for HBD-peptide (AALSLEEPAALAP) were synthesized by the Protein Chemistry Core Facility at the University of North Carolina. Purity and sequence confirmation were determined by mass spectrometry. The synthetic peptide for heparin-binding domain of IGFBP5 (²⁰¹RKGFYKRKQCKPSRGRKR²¹⁸) was also generated using the same method as mentioned above. The IGFBP2-HBD-peptide was pegylated as follows: 10 mg of peptide was mixed with 380 μ g of methoxy PEG maleimide (20000 kDa)(1:3 molar ratio peptide to PEG)(Jenkem

Biotechnology) in 4.0 ml of 0.05 M NaPO₄, pH 7.0. Following an overnight incubation at 4 °C, cysteine was added to a final concentration of 17 mM to block untreated sites. To remove the nonpegylated peptide and cysteine the mixture was desalted using a Zebra Desalt spin column (Thermo scientific) following the manufacturer's instruction. Pegylation was verified by SDS-PAGE analysis with Coomassie staining.

In vitro IGFBP-2 binding assay

Cells were starved with serum-free medium (SFM) overnight and then exposed to 0 or 50 ng/ml IGF-I for 10 min. They were suspended in 100 µl of PBS (pH 7.4) and incubated with biotinylated BP2 (final concentration of 28nM) and/or HBD (140 nM) for 4 hrs at 4 °C. The cells were washed three times with PBS and lysed with RIPA buffer. The cell lysates were centrifuged at 14,000 × g for 10 min at 4 °C. The proteins from supernatants were separated by 12.5% of SDS-PAGE and detected using horseradish peroxidase (HRP) conjugated avidin.

In vivo treatment of Igfbp2^{-/-} mice with pegylated heparin-binding peptide (PEG-HBD-peptide)-Igfbp2^{-/-} mice were administered with PBS or PEG-HBD-peptide (50 µg/day) intraperitoneally 5 times per week from 6 to 9 weeks of age. Dual-energy x-ray absorptiometry was performed before the initiation of treatment. Mice were injected with 20 mg/kg calcein intraperitoneally 7 days and 2 days before sample collection.

Dual-energy X-ray absorptiometry (DXA)-Dual-energy X-ray absorptiometry (DXA) for whole body and femoral areal bone mineral density (aBMD, g/cm²) and body composition exclusive of the head were performed using the PIXImus (GE-Lunar) as previously described (10).

MicroCT-Microarchitecture of distal trabecular bone and midshaft cortical bone were analyzed with femurs and vertebrae (L5) by high resolution microcomputed tomography (MicroCT40, Scanco Medical AG, Switzerland). Approximately 100 CT slices were measured just proximal to the distal growth plate, using an isotropic voxel size of 12 µm. Midshaft cortical bone properties were analysed in a similar fashion using 18 CT slices obtained at the mid-femoral diaphysis

BoneHistomorphometry-*In vivo* histomorphometry differences were analyzed between Igfbp2^{-/-} mice treated with PBS or PEG-HBD-peptide at 9 weeks of age. Mice were injected with 20 mg/kg calcein

intraperitoneally 7 days and 2 days before sample collection. Femurs were analyzed as described previously (10).

Femoral Biomechanics-Femoral biomechanical properties were compared by three-point bending between Igfbp2^{-/-} mice treated with PBS or PEG-HBD-peptide at 9 weeks of age. Load was applied at a constant rate (0.05 mm/sec) until failure. We measured maximum load (Newtons, N), bending stiffness (N/mm), and work-to-failure (N-mm) from the load-displacement curve and computed the apparent elastic modulus (GPa) and ultimate strength (GPa) using the relevant midfemoral cross-sectional geometry measured from µCT.

In vivo BrdU assay-BrdU (100 µg/gBW) and FdU (12 µg/gBW) were injected intraperitoneally in 2-week old male mice. 2 hours after of injection femurs were collected and fixed in 4% PFA overnight at 4°C. Femurs were decalcified using 15% EDTA (pH 7.4) for 5 days and sectioned. Endogenous peroxidase was blocked with 0.3% H₂O₂ in PBS and the sections were incubated with a mouse monoclonal anti-BrdU antibody (1:200, Sigma B8434) overnight at 4°C. The sections were then incubated with a biotinylated goat anti-mouse secondary antibody, followed by the incubation with streptavidin-biotinylated HRP complex and visualized with 3, 3'-diaminobenzidine.

Statistical analysis-All data are expressed as the mean ± Standard Error of the Mean (SEM). Results were analyzed for statistically significant differences using Student's *t*-test or ANOVA followed by Bonferroni multiple comparison *post hoc* test. Statistical significance was set at *p*<0.05.

Results

The heparin-binding domain of IGFBP-2 stimulates in vitro osteoblastogenesis. Previously, we reported that male Igfbp2^{-/-} mice exhibited an osteopenic phenotype with low bone formation and that osteoblastogenesis was impaired in bone marrow stromal cells (BMSCs) from Igfbp2^{-/-} mice compared to wild-type cells. Interestingly, male Igfbp2^{-/-} mice have a profound reduction in osteoblast number that accounts for the reduction in bone volume fraction in the tibia and femur although the percent of osteoblast apoptosis by Tunel staining did not differ between Igfbp2^{-/-} and

Igfbp2^{+/+}. To investigate whether the heparin-binding domain (HBD) of IGFBP-2 could be responsible for the phenotype of the *Igfbp2*^{-/-} mouse, we generated a synthetic peptide (the HBD-peptide) that does not bind IGFs, and which contains the HBD of IGFBP-2, and tested its effect on osteoblastogenesis *in vitro*. To confirm the specificity of the HBD-peptide, we also made a control peptide and analyzed its effect on osteogenesis. The control peptide did not enhance mineralization of *Igfbp2*^{-/-} COBs compared to PBS-treated cells, whereas the HBD-peptide stimulated COB mineralization (Figure 1A). Based on this, PBS was used as controls for further studies. To prolong the half-life of the HBD-peptide such that it was feasible to undertake *in vivo* studies, pegylation of the HBD-peptide was performed (PEG-HBD). *Igfbp2*^{-/-} COBs and BMSCs were cultured in osteogenic media in the presence of PBS, PEG-HBD or HBD-peptide. Both PEG-HBD and HBD-peptide enhanced osteogenesis as measured by alkaline phosphatase and Alizarin Red staining (Figures 1A-C). Consistent with this, *ALP*, *Runx2* and *osteocalcin* (*OC*) expression were enhanced in BMSCs treated with PEG-HBD vs PBS-treated cells (Figure 1D). Thus, there was no difference between the pegylated form of HBD and the HBD itself in respect to induction of osteogenesis.

The heparin-binding domain of IGFBP-2 stimulates periosteal expansion of metacarpals ex vivo. To further understand the anabolic effect of HBD on the skeleton, we next collected metacarpals from 1 day old mice, incubated them with osteogenic media in the absence of fetal calf serum and tested the effects of the HBD-peptide on osteogenesis. Bone accrual was evaluated by the longitudinal length of the calcein incorporated area as well as the width and length of the whole metacarpals. The control peptide had no effect on calcein incorporated area, and the length and width of the whole metacarpals were comparable to the metacarpals treated with PBS (Figures 1E-H). Hence PBS was used as the control for further studies. IGFBP-2 and the HBD-peptide significantly enhanced the calcein incorporated area of metacarpals (Figures 1I and J). IGF-I also stimulated expansion of the calcein incorporated area to a similar extent as IGFBP-2 and the HBD-peptide (Figures 1I and J). When metacarpals were treated with IGF-I together with the HBD-peptide,

the metacarpals displayed further enhancement of the calcein incorporated area (Figures 1I and J). In addition, IGFBP-2 and HBD-peptide also increased the width of the whole metacarpals, implying that IGFBP-2 has an important role in periosteal expansion (Figures 1K and L).

Because other IGFBPs possess HBD regions as well as IGFBP-2, we analyzed whether the osteogenic effect of the HBD is specific for this region in IGFBP-2 or whether the HBD in other forms of IGFBPs also had this effect. For this purpose we prepared a peptide that contained the HBD region of IGFBP-5 (BP5-HBD) in which the amino acid sequence is quite similar to the HBD in the C-terminal region of IGFBP-2 and determined its effect on osteogenesis. We cultured *Igfbp2*-deficient COBs in the presence of BP5-HBD and found that BP5-HBD did not show any enhancement of differentiation or mineralization compared to PBS-treated cells (Figure 2A). Second, we collected metacarpals and cultured them in osteogenic media with or without BP5-HBD. BP5-HBD had no effect on the calcein incorporated area, length or width of whole metacarpals (Figures 2B-E). These data suggest that the effect of the HBD on skeletal acquisition is likely specific to IGFBP-2.

The HBD of IGFBP-2 increases bone mass in growing Igfbp2^{-/-} mice. Next, we tested whether the HBD-peptide could enhance bone mass *in vivo*. After calculating the half-life of PEG-HBD (data not shown) *in vivo*, we administered 50 µg of PEG-HBD 5 times per week for 3 weeks to *Igfbp2*^{-/-} mice starting at 6 weeks of age. Because administration of pegylated control peptide in female C57BL/6J mice did not show any difference in terms of the change in areal bone mineral density (aBMD) compared with the treatment with PBS, PBS was used as a control in the *in vivo* study (Supplemental Figure S1). We first analyzed whether PEG-HBD could reverse the bone loss observed in the *Igfbp2*^{-/-} male mice. At baseline aBMD and bone mineral content (aBMC)/BW did not differ between *Igfbp2*^{-/-} mice treated with PBS or PEG-HBD (Supplemental Table S1). As expected, *Igfbp2*^{+/+} mice treated with PBS had higher trabecular bone volume by microCT compared to PBS-treated *Igfbp2*^{-/-} mice (Table 1). In *Igfbp2*^{-/-} mice, 3-week treatment with PEG-HBD enhanced aBMD and aBMC/BW compared to PBS, although it did not reach a

statistical significance (Supplemental Table S1). MicroCT revealed a higher trabecular bone volume fraction and greater trabecular thickness in both the distal femur and L5 vertebrae of *Igfbp2*^{-/-} mice treated with PEG-HBD vs PBS-treated *Igfbp2*^{-/-} mice. (Figure 3A, Tables 1 and 2). At the femoral midshaft, cortical thickness was not affected by PEG-HBD treatment, but total bone area was increased in PEG-HBD treated *Igfbp2*^{-/-} mice vs PBS-treated *Igfbp2*^{-/-} mice (Table 1). This is consistent with an effect of PEG-HBD on periosteal expansion which was also noted in the metacarpal assay. The cortical bone changes were associated with a modest albeit non-significant increase in strength parameters analyzed by a three-point bending assay (Supplemental Figure S2). In addition, 3-week treatment with PEG-HBD did not have any effect on the width and morphology of growth plate, which is consistent with the *ex vivo* metacarpal culture findings that the HBD did not affect the length of whole metacarpals (Supplemental Figure S3).

Dynamic histomorphometry revealed that osteoblast number per bone perimeter was increased 33% in PEG-HBD treated *Igfbp2*^{-/-} mice vs PBS-treated *Igfbp2*^{-/-} mice, whereas osteoclast number showed a trend toward a decrease in the PEG-HBD treated *Igfbp2*^{-/-} mice vs PBS-treated *Igfbp2*^{-/-} mice (Table 3). Consistent with the increase in osteoblast number in HBD-treated mice, *in vivo* BrdU labeling of the femur in *Igfbp2*^{-/-} mice revealed significantly enhanced proliferation of osteoblasts in the HBD-treated *Igfbp2*^{-/-} group compared to PBS treated *Igfbp2*^{-/-} mice; furthermore the degree of BrdU labeling in the HBD treated group was the same as that of PBS-treated *Igfbp2*^{+/+} mice (Figure 3B).

Consistent with the decreased number of osteoclasts, serum TRAP5b levels were significantly decreased in PEG-HBD treated *Igfbp2*^{-/-} mice (Figure 3C). However, PEG-HBD or HBD-peptide did not directly affect osteoclastogenesis in *Igfbp2*^{-/-} bone marrow cells (data not shown), although PEG-HBD suppressed *Rankl* expression without changing *Opg* expression in *Igfbp2*^{-/-} COBs (Figures 3D and E). The number of bone marrow adipocytes was reduced in PEG-HBD treated *Igfbp2*^{-/-} mice although whole body adiposity was unchanged (Figure 3F, Supplemental Table S1). Not surprisingly, bone marrow *Pparg* expression was

significantly reduced in COBs treated with PEG-HBD (Figure 3G).

We previously reported that female *Igfbp2*^{-/-} mice exhibited a different phenotype from male *Igfbp2*^{-/-} mice in that no trabecular bone differences were noted in *Igfbp2*^{-/-} female mice compared to littermate controls (10). Based on these observations, we analyzed whether PEG-HBD still had a positive effect on skeletal mass in female *Igfbp2*^{-/-} mice even in the absence of a skeletal phenotype. At baseline, whole body aBMD and aBMC/BW were not different between female *Igfbp2*^{-/-} mice treated with PBS or PEG-HBD (Supplemental Table S2). Interestingly, PEG-HBD significantly increased whole body aBMD and aBMC/BW compared to PBS-treatment (Supplemental Table S2). MicroCT confirmed that the skeletal phenotype in response to PEG-HBD was very similar to what was observed in *Igfbp2*^{-/-} males; i.e. enhanced cortical bone size and increased trabecular bone volume (Table 4). However, unlike the *Igfbp2*^{-/-} male mice, the increase in trabecular volume fraction was associated with increased trabecular number rather than thickness. These lines of evidence imply that the HBD not only rescues the low bone mass phenotype of growing *Igfbp2*^{-/-} male mice, but also possesses an intrinsic anabolic effect during skeletal acquisition.

The heparin-binding domain of IGFBP-2 suppresses PTEN expression and stimulates IGF-I/Akt signaling. There is evidence of a negative association between IGFBP-2 and PTEN expression in human cancer cells such as glioblastoma and prostate cancer (19-21,25). In addition, we have shown that PTEN expression was enhanced in *Igfbp2*-deficient osteoblasts (10). These findings led us to speculate that IGFBP-2 negatively regulates PTEN expression and enhances IGF-I signaling in osteoblasts. First we analyzed whether IGFBP-2 suppressed PTEN expression using primary *Igfbp2*^{-/-} COBs and found that full-length IGFBP-2 suppressed PTEN expression in these cells (Figures 4A and B). The control peptide had no effect on PTEN expression (Figures 4C and D), but much like IGFBP-2, the HBD-peptide and PEG-HBD also induced a reduction in PTEN expression in a dose and time dependent manner (Figures 4C-H). Second, we asked whether the reduction in PTEN expression resulted in enhanced IGF-I/Akt signaling. Western

blot analysis for phosphorylation of Akt at serine 473 (pSer473-Akt) revealed that IGF-I stimulated Akt activation was impaired in *Igfbp2*^{-/-} COBs compared to *Igfbp2*^{+/+} COBs (Figures 4I and J). Furthermore, pSer473-Akt was enhanced in *Igfbp2*^{-/-} COBs treated with PEG-HBD vs PBS-treated controls (Figures 4K and L). The effects of PEG-HBD on PTEN suppression and Akt phosphorylation by IGF-I were weaker than those of full-length IGFBP-2 protein (Figure 4M). To examine which Akt isoform is involved in this process, we analyzed the expression of Akt1 and Akt2 in COBs. As shown in Figure 4N, both Akt1 and Akt2 are expressed in this cell type. Interestingly, although Ser473 phosphorylation of Akt1 by IGF-I was impaired in *Igfbp2*^{-/-} COBs, Akt2 phosphorylation by IGF-I was not changed after being adjusted by the expression of total Akt2 (Figure 4N).

Finally, we investigated whether the heparin binding domain of IGFBP-2 is required for the suppression of PTEN expression by IGFBP-2. For this purpose, we performed an *in vitro* binding assay to test whether IGFBP-2 can interact with COBs using biotinylated IGFBP-2 and found that IGFBP-2 binds to the cell surface of COBs, which was further enhanced in the presence of IGF-I (Figure 4O). In addition, the binding of IGFBP-2 to the cell surface of COBs was partially blocked in the presence of PEG-HBD (Figure 4O). These data indicate that IGFBP-2 enhances IGF-I stimulated/Akt activation, by suppressing PTEN expression in part through its HBD, thereby further activating Akt1.

The heparin-binding domain of IGFBP-2 stimulates IGF-I induced cytosolic β -catenin accumulation and Ser552 phosphorylation of β -catenin. Several lines of evidence demonstrate cross-talk between IGF-I signaling and β -catenin signaling in tumor cell lines (26-29). Thus, we hypothesized that IGF-I signaling would stimulate β -catenin signaling and that HBD-peptide could enhance β -catenin signaling by suppressing PTEN expression in osteoblastic cells. We analyzed whether IGF-I affects β -catenin accumulation in the cytosol of osteoblastic cells. Western blot analysis revealed that IGF-I enhanced cytosolic accumulation of β -catenin associated with the reduced expression of membrane β -catenin in MC3T3-E1 cells (Figure 5A). In addition,

cytosolic accumulation of β -catenin in response to IGF-I was enhanced in *Igfbp2*^{-/-} COBs treated with PEG-HBD compared to PBS-treated control cells (Figures 5B and C). This suggests that the HBD-peptide is involved in IGF-I/ β -catenin signaling possibly by suppressing PTEN expression. Serine 552 (Ser552) phosphorylation of β -catenin, which can be induced by Akt, has been shown to be important for dissociation of β -catenin from membrane and re-localization to cytoplasm and nucleus (30-32). Based on this observation, we asked whether IGF-I stimulated Ser552 phosphorylation in β -catenin and if the PEG-HBD facilitates this response in osteoblastic cells. As shown in Figures 5D-F, IGF-I stimulated β -catenin phosphorylation on Ser552 and this response was enhanced in cells treated with PEG-HBD. Because activation of β -catenin is important for bone formation, the osteogenic effect of the HBD-peptide might be mediated by IGF-I/ β -catenin signaling in osteoblasts (33).

Discussion

In this study, we report that IGFBP-2 has anabolic properties in the growing skeleton and that part of its biologic effect is mediated through the HBD in an IGF-binding independent manner. IGFBP-2 levels are very high during neonatal growth and again during pubertal bone acquisition. IGF-I is also a critical factor for bone accrual and it can induce IGFBP-2 expression in bone cells (34). Previous studies have shown that excess IGFBP-2 relative to IGF-I could inhibit the biologic activity of IGF-I (3). In line with this, an excess of IGFBP-2 has been shown to suppress osteoblast proliferation in part by antagonizing IGF-I action. *In vivo*, genetic models over-expressing *Igfbp2* have reduced body mass and bone size (7,35). In contrast, Khosla et al. reported that IGF-II in complex with IGFBP-2 (used in equimolar amounts) had a high affinity for bone matrix, stimulated osteoblast proliferation, and could prevent disuse osteoporosis (8,9). Palermo et al. also showed that lower concentrations of IGFBP-2 stimulated IGF-II induced ALP expression in rat tibial osteoblasts (34). In this study we expanded our insights into the physiologic role of IGFBP-2 and provide new evidence that the heparin-binding domain of

IGFBP-2 may enhance bone mass principally by stimulating osteoblast proliferation.

Initially we characterized the skeletal phenotype of male *Igfbp2*^{-/-} mice and found decreased skeletal mass, reduced numbers of osteoblasts and low bone turnover (10). These findings suggested that physiological concentrations of IGFBP-2 were required for recruitment of osteoblasts and proper bone acquisition. Because forming a protein complex with IGFBP-2 is critical for stabilization of IGF-I in the pericellular space, an anabolic action for IGFBP-2 was certainly conceivable particularly when the anabolic effects of IGF-I were considered within that same context. Furthermore emerging evidence suggests that IGFBP-2 could function at least partially independent of IGF-I binding to stimulate cell proliferation through the HBD domain that mediates IGFBP-2 binding to the extracellular matrix (13-16). Consistent with this tenet, we demonstrated that IGFBP-2 binding to the cell surface was partially blocked in the presence of HBD-peptide. Importantly, IGFBP-2 binding to the cell surface was greatly enhanced in the presence of IGF-I, suggesting that the native protein may have undergone a conformational change following IGF-I association.

Our finding that the HBD suppresses PTEN in osteoblasts, and enhances osteoblast proliferation provides a possible mechanism by which IGFBP-2 could regulate skeletal mass, in coordination with IGF-I. This may be particularly relevant during stages of rapid bone growth such as the neonatal and adolescent period when the recruitment of osteoblast precursors is critical. However, sorting the IGF-I- dependent and independent activities of intact IGFBP-2 is challenging. Clearly, IGF-I signaling is a prerequisite for skeletal acquisition. Furthermore, we and others have shown that modulation of the IGF signaling pathway results in alterations in skeletal homeostasis (18,36-41). Therefore, an anabolic effect of the HBD on the skeleton could in part be mediated by enhanced IGF-I-induced activation of the PI3K/Akt pathway as a result of PTEN suppression. In addition, the increase in osteoblast number in HBD-treated *Igfbp2*^{-/-} mice could also be due to this mechanistic change since enhanced PI3K/Akt signaling in osteoblasts is involved in cell proliferation. In fact, Liu et al. showed that loss of PTEN in osteoblasts *in vivo*

resulted in very high bone mass and increased osteoblast number (18).

Although administration of the HBD rescued the low osteoblast number in *Igfbp2*^{-/-} mice, osteoclast number was further diminished by administration of HBD. This observation is consistent with the observed increase in bone mass but suggests that bone turnover is not accelerated by HBD treatment. Indeed, mineral apposition rate and bone formation rate showed minimal changes in *Igfbp2*^{-/-} mice treated with HBD. In contrast to the HBD, IGF-I signaling has been shown to directly stimulate osteoclastogenesis (42) and our prior data suggest that physiological levels of IGFBP-2 in the skeletal microenvironment are required for osteoclastogenesis. It is very possible that IGFBP-2 acts to maintain IGF-I concentrations within the pericellular niche but that the HBD which lacks the IGF-I binding domain may play a distinct role by inhibiting bone resorption when supraphysiologic concentrations are administered. Since the HBD does not directly suppress osteoclast differentiation *in vitro*, the underlying mechanism whereby the HBD decreases bone resorption is likely indirect and due to decreased *Rankl* expression in osteoblasts.

A reduction in PTEN expression has been shown to be associated with increased β -catenin signaling. Inactivation of GSK3 β (glycogen synthase kinase 3) by Akt has been proposed to be the key pathway by which Akt activation enhances β -catenin stabilization, whereas several lines of evidence demonstrates the important role of Ser552 phosphorylation in β -catenin activation (30-32). β -catenin is directly phosphorylated by Akt and Ser552 phosphorylation is important for cytosolic and nuclear accumulation of β -catenin, resulting in increased β -catenin transcriptional activity (30). He et al reported that loss of PTEN resulted in an excess of intestinal stem cells by stimulating β -catenin activity in part through Ser552 phosphorylation (31). In the current study we demonstrated that IGF-I enhanced β -catenin accumulation in cytoplasm and phosphorylated Ser552 of β -catenin in osteoblastic cells, and this response was further enhanced by addition of the HBD. Taken together, these lines of evidence support our findings of a synergistic effect of IGFBP-2 with IGF-I on β -catenin signaling and suggest that the increased bone formation noted in

Igfbp2^{-/-} mice treated with PEG-HBD is related to activation of this signaling pathway.

In the PEG-HBD treated *Igfbp2*^{-/-} mice, cell proliferation (as measured by BrdU labeling) and osteoblast number by histomorphometry were increased and were accompanied by reduced number of marrow adipocytes. Mesenchymal cell allocation is an important step in regulating bone mass and marrow adiposity. Numerous factors are involved in this process including Wnt/ β -catenin signaling and the transcription factor, PPAR-gamma (43). Activation of Wnt/ β -catenin signaling favors osteoblastogenesis over adipogenesis in part by either sequestering PPAR-gamma or suppressing PPAR-gamma transcriptional activity (44-46). Because HBD enhances β -catenin stability that is induced by IGF-I, the switch of mesenchymal cells towards the osteogenic lineage might explain the increased cell proliferation as well as osteoblast number and reduced adipocyte number in bone marrow from *Igfbp2*^{-/-} mice treated with PEG-HBD.

Nevertheless, the mechanism by which the HBD suppresses PTEN expression has not been defined. One possibility resides in the binding of HBD with the integrin receptor. Maile et al. reported that heparin-binding domain of vitronectin bound to a cystein loop region of β 3 integrin and modulated α V β 3 integrin signaling in smooth muscle cells (47). Furthermore, Perks et al. reported that PTEN down-regulation by IGFBP-2 might be mediated by an integrin receptor, although they did not demonstrate an interaction between IGFBP-2 and a specific integrin receptor or whether the HBD was involved in this interaction (20). Further studies are needed to define specific sites of IGFBP-2 binding leading to activation of two critical intracellular signaling pathways.

Our results using supraphysiologic concentration of the HBD cannot be used to reach

a definitive conclusion regarding the role of physiologic concentrations of IGFBP-2 in bone acquisition, particularly relative to IGF-I. However, it does suggest that this binding protein has unique properties that might explain the high circulating levels of IGFBP-2 during periods of rapid growth such as the first year of life and during puberty, a time when serum IGF-I levels are also high. Importantly, HBD increased bone mass even in growing female mice that do not have alterations in bone mineral density (10). Further analyses are needed to determine whether HBD also has an anabolic effect in older mice. Notwithstanding, we found that the HBD in IGFBP-2 has an anabolic effect on the skeleton of growing mice by targeting osteoblast recruitment through suppression of PTEN expression and activation of β -catenin signaling. These data support the tenet that IGFBP-2, which is induced by IGF-I could act synergistically with IGF-I to promote cell proliferation through its unique heparin binding domain in the linker region of the molecule. Our studies lend further support to recent work from the Lodish laboratory demonstrating the strong proliferative properties of IGFBP-2 in hematopoietic stem cells (11) and provide a potential mechanism for IGFBP-2 activity in some neoplasms.

In summary, we show that the HBD in IGFBP-2 has an anabolic effect on the skeleton and this effect is mediated by the suppression of PTEN expression and involves activation of β -catenin signaling. These lines of evidence add to our growing knowledge regarding the physiologic role of IGFBP-2 relative to IGF-I in several tissues and provide insights into the cross-talk between two signaling networks that have been shown to be essential for bone growth and maintenance.

References

1. Hwa, V., Oh, Y., and Rosenfeld, R. G. (1999) *Endocr Rev* **20**(6), 761-787
2. Jones, J. I., and Clemmons, D. R. (1995) *Endocr Rev* **16**(1), 3-34
3. Firth, S. M., and Baxter, R. C. (2002) *Endocr Rev* **23**(6), 824-854
4. Hu, D., Pawlikowska, L., Kanaya, A., Hsueh, W. C., Colbert, L., Newman, A. B., Satterfield, S., Rosen, C., Cummings, S. R., Harris, T. B., and Ziv, E. (2009) *J Am Geriatr Soc* **57**(7), 1213-1218
5. Hedbacker, K., Birsoy, K., Wysocki, R. W., Asilmaz, E., Ahima, R. S., Farooqi, I. S., and Friedman, J. M. *Cell Metab* **11**(1), 11-22
6. Wheatcroft, S. B., Kearney, M. T., Shah, A. M., Ezzat, V. A., Miell, J. R., Modo, M., Williams, S. C., Cawthorn, W. P., Medina-Gomez, G., Vidal-Puig, A., Sethi, J. K., and Crossey, P. A. (2007) *Diabetes* **56**(2), 285-294
7. Hoeflich, A., Nedbal, S., Blum, W. F., Erhard, M., Lahm, H., Brem, G., Kolb, H. J., Wanke, R., and Wolf, E. (2001) *Endocrinology* **142**(5), 1889-1898
8. Conover, C. A., Johnstone, E. W., Turner, R. T., Evans, G. L., John Ballard, F. J., Doran, P. M., and Khosla, S. (2002) *Growth Horm IGF Res* **12**(3), 178-183
9. Khosla, S., Hassoun, A. A., Baker, B. K., Liu, F., Zein, N. N., Whyte, M. P., Reasner, C. A., Nippoldt, T. B., Tiegs, R. D., Hintz, R. L., and Conover, C. A. (1998) *J Clin Invest* **101**(10), 2165-2173
10. DeMambro, V. E., Clemmons, D. R., Horton, L. G., Bouxsein, M. L., Wood, T. L., Beamer, W. G., Canalis, E., and Rosen, C. J. (2008) *Endocrinology* **149**(5), 2051-2061
11. Zhang, C. C., Kaba, M., Iizuka, S., Huynh, H., and Lodish, H. F. (2008) *Blood* **111**(7), 3415-3423
12. Arai, T., Busby, W., Jr., and Clemmons, D. R. (1996) *Endocrinology* **137**(11), 4571-4575
13. Russo, V. C., Bach, L. A., Fosang, A. J., Baker, N. L., and Werther, G. A. (1997) *Endocrinology* **138**(11), 4858-4867
14. Russo, V. C., Rekaris, G., Baker, N. L., Bach, L. A., and Werther, G. A. (1999) *Endocrinology* **140**(7), 3082-3090
15. Russo, V. C., Schutt, B. S., Andaloro, E., Ymer, S. I., Hoeflich, A., Ranke, M. B., Bach, L. A., and Werther, G. A. (2005) *Endocrinology* **146**(10), 4445-4455
16. Duan, C., Ding, J., Li, Q., Tsai, W., and Pozios, K. (1999) *Proc Natl Acad Sci U S A* **96**(26), 15274-15279
17. Kawai, M., and Rosen, C. J. (2009) *Pediatr Nephrol* **24**(7), 1277-1285
18. Liu, X., Bruxvoort, K. J., Zylstra, C. R., Liu, J., Cichowski, R., Faugere, M. C., Bouxsein, M. L., Wan, C., Williams, B. O., and Clemens, T. L. (2007) *Proc Natl Acad Sci U S A* **104**(7), 2259-2264
19. Mehrian-Shai, R., Chen, C. D., Shi, T., Horvath, S., Nelson, S. F., Reichardt, J. K., and Sawyers, C. L. (2007) *Proc Natl Acad Sci U S A* **104**(13), 5563-5568
20. Perks, C. M., Vernon, E. G., Rosendahl, A. H., Tonge, D., and Holly, J. M. (2007) *Oncogene* **26**(40), 5966-5972
21. Levitt, R. J., Georgescu, M. M., and Pollak, M. (2005) *Biochem Biophys Res Commun* **336**(4), 1056-1061
22. Sakata, T., Wang, Y., Halloran, B. P., Elalieh, H. Z., Cao, J., and Bikle, D. D. (2004) *J Bone Miner Res* **19**(3), 436-446
23. Shoba, L. N., and Lee, J. C. (2003) *J Cell Biochem* **88**(6), 1247-1255
24. Wood, T. L., Rogler, L. E., Czick, M. E., Schuller, A. G., and Pintar, J. E. (2000) *Mol Endocrinol* **14**(9), 1472-1482
25. Cohen, P., Peehl, D. M., Stamey, T. A., Wilson, K. F., Clemmons, D. R., and Rosenfeld, R. G. (1993) *J Clin Endocrinol Metab* **76**(4), 1031-1035
26. Jin, T., George Fantus, I., and Sun, J. (2008) *Cell Signal* **20**(10), 1697-1704

27. Desbois-Mouthon, C., Cadoret, A., Blivet-Van Eggelpoel, M. J., Bertrand, F., Cherqui, G., Perret, C., and Capeau, J. (2001) *Oncogene* **20**(2), 252-259
28. Playford, M. P., Bicknell, D., Bodmer, W. F., and Macaulay, V. M. (2000) *Proc Natl Acad Sci U S A* **97**(22), 12103-12108
29. Amin, S., Riggs, B. L., Melton, L. J., 3rd, Achenbach, S. J., Atkinson, E. J., and Khosla, S. (2007) *J Bone Miner Res* **22**(6), 799-807
30. Fang, D., Hawke, D., Zheng, Y., Xia, Y., Meisenhelder, J., Nika, H., Mills, G. B., Kobayashi, R., Hunter, T., and Lu, Z. (2007) *J Biol Chem* **282**(15), 11221-11229
31. He, X. C., Yin, T., Grindley, J. C., Tian, Q., Sato, T., Tao, W. A., Dirisina, R., Porter-Westpfahl, K. S., Hembree, M., Johnson, T., Wiedemann, L. M., Barrett, T. A., Hood, L., Wu, H., and Li, L. (2007) *Nat Genet* **39**(2), 189-198
32. Taurin, S., Sandbo, N., Qin, Y., Browning, D., and Dulin, N. O. (2006) *J Biol Chem* **281**(15), 9971-9976
33. Glass, D. A., 2nd, and Karsenty, G. (2006) *Curr Top Dev Biol* **73**, 43-84
34. Palermo, C., Manduca, P., Gazzerro, E., Foppiani, L., Segat, D., and Barreca, A. (2004) *Am J Physiol Endocrinol Metab* **286**(4), E648-657
35. Eckstein, F., Pavicic, T., Nedbal, S., Schmidt, C., Wehr, U., Rambeck, W., Wolf, E., and Hoeflich, A. (2002) *Anat Embryol (Berl)* **206**(1-2), 139-148
36. Fujita, T., Azuma, Y., Fukuyama, R., Hattori, Y., Yoshida, C., Koida, M., Ogita, K., and Komori, T. (2004) *J Cell Biol* **166**(1), 85-95
37. Peng, X. D., Xu, P. Z., Chen, M. L., Hahn-Windgassen, A., Skeen, J., Jacobs, J., Sundararajan, D., Chen, W. S., Crawford, S. E., Coleman, K. G., and Hay, N. (2003) *Genes Dev* **17**(11), 1352-1365
38. Liu, J. P., Baker, J., Perkins, A. S., Robertson, E. J., and Efstratiadis, A. (1993) *Cell* **75**(1), 59-72
39. Yakar, S., Rosen, C. J., Beamer, W. G., Ackert-Bicknell, C. L., Wu, Y., Liu, J. L., Ooi, G. T., Setser, J., Frystyk, J., Boisclair, Y. R., and LeRoith, D. (2002) *J Clin Invest* **110**(6), 771-781
40. Zhang, M., Xuan, S., Bouxsein, M. L., von Stechow, D., Akeno, N., Faugere, M. C., Malluche, H., Zhao, G., Rosen, C. J., Efstratiadis, A., and Clemens, T. L. (2002) *J Biol Chem* **277**(46), 44005-44012
41. Zhao, G., Monier-Faugere, M. C., Langub, M. C., Geng, Z., Nakayama, T., Pike, J. W., Chernausek, S. D., Rosen, C. J., Donahue, L. R., Malluche, H. H., Fagin, J. A., and Clemens, T. L. (2000) *Endocrinology* **141**(7), 2674-2682
42. Wang, Y., Nishida, S., Elalieh, H. Z., Long, R. K., Halloran, B. P., and Bikle, D. D. (2006) *J Bone Miner Res* **21**(9), 1350-1358
43. Gesta, S., Tseng, Y. H., and Kahn, C. R. (2007) *Cell* **131**(2), 242-256
44. Liu, J., Wang, H., Zuo, Y., and Farmer, S. R. (2006) *Mol Cell Biol* **26**(15), 5827-5837
45. Bennett, C. N., Longo, K. A., Wright, W. S., Suva, L. J., Lane, T. F., Hankenson, K. D., and MacDougald, O. A. (2005) *Proc Natl Acad Sci U S A* **102**(9), 3324-3329
46. Ross, S. E., Hemati, N., Longo, K. A., Bennett, C. N., Lucas, P. C., Erickson, R. L., and MacDougald, O. A. (2000) *Science* **289**(5481), 950-953
47. Maile, L. A., Aday, A. W., Busby, W. H., Sanghani, R., Veluvolu, U., and Clemmons, D. R. (2008) *J Cell Biochem* **105**(2), 437-446

Footnotes

M.K., D.R.C, and C.J.R. conceived and designed the experiments. M.K. performed the majority of the experiments. E.C. helped with the histomorphometric analysis. M.L.B assisted with the bone breaking experiments. All of the authors analyzed the data. M.K. and C.J.R. wrote the paper.

This work is supported by the grant from NIH AR021707 (E.C.). Abbreviations used are: ALP: alkaline phosphatase, Runx2: Runt-related transcription factor 2, PPAR-gamma: Peroxisome proliferators-activated receptor-gamma, RANKL: Receptor activator of NF-kappa B ligand, OPG: Osteoprotegerin.

Figure legends

Fig. 1. The heparin-binding domain of IGFBP-2 enhances osteoblastogenesis *in vitro* and *ex vivo*. A. *Igfbp2*^{-/-} calvarial osteoblasts (COBs) were cultured with osteogenic media with PBS, control peptide (2 µg/ml) or the heparin-binding domain peptide (HBD-peptide) (2 µg/ml). Osteoblastogenesis was evaluated by Alizarin Red staining. B-D. *Igfbp2*^{-/-} COBs and bone marrow stromal cells (BMSCs) were treated with osteogenic media with pegylated heparin-binding domain peptide (PEG-HBD) (2 µg/ml). ALP staining (day 7) and Alizarin Red staining (day 14) were performed (B). Alizarin Red staining positive area was quantified using NIH image (C). Expression of *ALP*, *osteocalcin (OC)* and *Runx2* was analyzed by real-time RT-PCR using BMSCs at day 14 (n=3) (D). E-L. *Igfbp2*^{-/-} metacarpals were treated with osteogenic media with PBS or control peptide (2 µg/ml) (E-H). *Igfbp2*^{-/-} metacarpals were treated with osteogenic media with IGFBP-2 (200 ng/ml) or the heparin-binding domain peptide (HBD-peptide) (2 µg/ml) in the presence or absence of IGF-1 (20 ng/ml)(I-L). At day 10, bones were treated with 500 ng/ml of calcein for 2 hours. The calcein incorporated area was visualized (E, I), and longitudinal length of the calcein incorporated area was quantified (F, J). Metacarpals were fixed with 4% PFA and subjected to Alcian blue and von Kossa double staining (G, K). The length and width of the whole metacarpals were quantified (H, L) Figures shown represent at least 3 independent experiments. Values are expressed as the mean ± SEM (n=3-4). * p<0.05, ^a p<0.05 vs PBS, ^b p<0.01 vs PBS, ^c p<0.001 vs PBS, ^d p<0.01 vs HBD-peptide, ^e p<0.05 vs IGF-I, ^f p<0.05 vs HBD-peptide, ns; not significant.

Fig. 2. The heparin-binding domain of IGFBP-5 does not show any effects on *in vitro* osteoblastogenesis or periosteal expansion of metacarpals *ex vivo*. A. *Igfbp2*^{-/-} primary calvarial osteoblasts were treated with osteogenic media with or without the heparin-binding domain of IGFBP-5 (BP5-HBD) (2 µg/ml). Osteoblastogenesis was evaluated by Alizarin Red staining. B-E. *Igfbp2*^{-/-} metacarpals were treated with osteogenic media with or without BP5-HBD (2 µg/ml) for 10 days. Bones were labeled with calcein (500 ng/ml) and the calcein incorporated area was visualized (B). Longitudinal length of calcein incorporated area was quantified (C). Alcian blue and Von Kossa double staining was performed (D) and the length and width of whole metacarpals were quantified (E). Figures shown represent at least 3 independent experiments. Values are expressed as the mean ± SEM (n=3). ns: not significant.

Fig. 3. The heparin-binding domain of IGFBP-2 enhances bone mass of *Igfbp2*^{-/-} mice. Male *Igfbp2*^{+/+} mice were treated with PBS and male *Igfbp2*^{-/-} mice were treated with PBS or pegylated heparin-binding domain (PEG-HBD) from 6 to 9 weeks (A, C and F). Two-week old male *Igfbp2*^{+/+} mice were treated with PBS and *Igfbp2*^{-/-} mice were treated with PBS or PEG-HBD (15 µg) for 3 days (B). A. MicroCT image of distal femur at 9-week old. B. BrdU staining was performed using the distal femur and the percentage of BrdU positive osteoblasts was calculated (n=3). C. Serum Trap5b levels were analyzed by ELISA in *Igfbp2*^{-/-} mice at 9-week old (n=6-9). D and E. *Igfbp2*^{-/-} calvarial osteoblasts (COBs) were treated with or without PEG-HBD for 2

hours (D). *Igfbp2*^{-/-} BMSCs were cultured with osteogenic media with PBS or PEG-HBD for 2 weeks (E). Expression of *Opg* and *Rankl* was analyzed by real-time RT-PCR (n=3). F. Adipocyte number was counted just proximal to the distal growth plate of femur and normalized by the total area (N.Ad/T.Ar) in *Igfbp2*^{-/-} mice at 9-week old (n=6). G. *Igfbp2*^{-/-} COBs were treated with PBS or PEG-HBD for 24 hours in serum-free media. Expression of *Pparg* was analyzed by real-time PCR (n=3). Figures shown represent at least 3 independent experiments. Values are expressed as the mean ± SEM. * p<0.001, ** p<0.01, † p<0.05.

Fig. 4. The heparin-binding domain of IGFBP-2 suppresses PTEN expression. A and B. *Igfbp2*^{-/-} calvarial osteoblasts (COBs) were treated with PBS, control peptide, or heparin-binding domain peptide (HBD-peptide) overnight, and whole cell lysate was collected. PTEN expression was analyzed using Western blot analysis (A), and quantitative analysis was performed (B). C-H. *Igfbp2*^{-/-} COBs were isolated and serum-starved overnight with PBS, IGFBP-2 (C and D) or pegylated heparin-binding domain peptide (PEG-HBD) at indicated concentration or period (E-H). Whole cell lysates were collected and expression of PTEN was analyzed by Western blot analysis. Expression levels of PTEN were quantified by normalizing to the expression levels of β-actin. I-L. *Igfbp2*^{+/+} or *Igfbp2*^{-/-} COBs were serum-starved overnight and treated with IGF-I (100 ng/ml) for 15 minutes (I and J). *Igfbp2*^{-/-} COBs were serum-starved with PBS or PEG-HBD overnight and treated with IGF-I (100 ng/ml) for 15 minutes (K and L). Whole cell lysates were collected and expression of pSer473-Akt (pAkt) and Akt was analyzed by Western blot analysis. Expression levels of pSer473-Akt were quantified by normalizing to the expression levels of Akt. M. *Igfbp2*^{-/-} COBs were exposed to IGF-I (50 ng/ml), IGFBP-2 (200 ng/ml) or the PEG-HBD (2 μg/ml) for 4 hrs. Lysates were prepared and immunoblotted for total PTEN or pAkt. Immunoblotting for β-actin is shown as a loading control. N. COBs were isolated from *Igfbp2*^{+/+} and *Igfbp2*^{-/-} mice. Duplicate cultures were exposed to IGF-I (50 ng/ml) for 10 min. The lysates were immunoprecipitated for Akt1 or Akt2 and then immunoblotted for pAkt or the respective Akt1 and Akt2 proteins. O. *Igfbp2*^{-/-} COBs were incubated with IGF-I (50 ng/ml), IGFBP-2 (200 ng/ml) or the PEG-HBD (2 μg/ml) in the various combinations shown. They were also exposed to biotinylated IGFBP-2. Cell lysates were prepared and analyzed by SDS-PAGE with immunoblotting using HRP Avidin. Figures shown represent at least 3 independent experiments. Values are expressed as the mean ± SEM (n=3-4). * p<0.001, ** p<0.01, † p<0.05.

Fig. 5. The heparin-binding domain of IGFBP-2 stimulates cytosolic accumulation and Ser552 phosphorylation of β-catenin by IGF-I. A. MC3T3-E1 cells were serum-starved overnight and treated with IGF-I at the indicated concentration for 6 hours. Expression of β-catenin was analyzed by Western blot analysis using membrane and cytosolic fraction. Pan-cadherin and β-actin was used as a loading control for membrane and cytosolic fraction, respectively. B and C. *Igfbp2*^{-/-} calvarial osteoblasts (COBs) were serum-starved overnight with PBS or pegylated heparin-binding domain peptide (PEG-HBD) and treated with IGF-I (100 ng/ml) for 6 hours. Expression of β-catenin was analyzed by Western blot analysis using cytosolic fraction (B) and quantified by normalizing to the expression levels of β-actin (C). D. MC3T3-E1 cells were serum-starved overnight and treated with IGF-I at the indicated concentration for 15 min. Expression of pSer552-β-catenin, β-catenin, pSer473-Akt (pAkt) and Akt was analyzed by Western blot analysis using whole cell lysates. E and F. *Igfbp2*^{-/-} COBs were serum-starved overnight with PBS or PEG-HBD and treated with IGF-I (100 ng/ml) for 15 min. Expression of pSer552-β-catenin was analyzed by Western blot analysis using whole cell lysates (E) and quantified by normalizing to the expression levels of β-catenin (F). Figures shown represent at least 3 independent experiments. Values are expressed as the mean ± SEM (n=3). * p<0.01, ** p<0.05.

Tables

Table 1. MicroCT analysis of femurs from PBS-treated IGFBP2^{+/+} and PBS or PEG-HBD peptide-treated IGFBP2^{-/-} male mice

	IGFBP2 ^{+/+} PBS N=8	IGFBP2 ^{-/-} PBS N=12	IGFBP2 ^{-/-} PEG-HBD N=6
Midshaft			
Cortical thickness (mm)	0.198 ± 0.007	0.197 ± 0.003	0.200 ± 0.006
Bone area (mm ²)	0.889 ± 0.047	0.868 ± 0.018	0.903 ± 0.024
Total area (mm ²)	1.970 ± 0.062	1.955 ± 0.036	2.076 ± 0.031 ^a
Bone area/Total area	0.449 ± 0.011	0.444 ± 0.006	0.435 ± 0.014
Distal Femur			
Bone volume/Total volume	0.143 ± 0.017	0.095 ± 0.007 ^b	0.125 ± 0.012 ^c
Trabecular number (1/mm)	4.86 ± 0.16	4.29 ± 0.09 ^b	4.47 ± 0.15
Trabecular thickness (mm)	0.047 ± 0.003	0.041 ± 0.001	0.048 ± 0.002 ^d
Trabecular spacing (mm)	0.200 ± 0.007	0.230 ± 0.005 ^b	0.221 ± 0.008

PEG-HBD; pegylated heparin-binding domain

Values are expressed as the mean ± SEM.

a: p<0.05 vs IGFBP2^{-/-} with PBS

b: p<0.01 vs IGFBP2^{+/+} with PBS

c: p<0.05 vs IGFBP2^{-/-} with PBS

d: p<0.01 vs IGFBP2^{-/-} with PBS

Table 2. MicroCT analysis of vertebrae (L5) from male *Igfbp2^{+/+}* treated with PBS and male *Igfbp2^{-/-}* treated with PBS or PEG-HBD

	<i>Igfbp2^{+/+}</i> PBS N=7	<i>Igfbp2^{-/-}</i> PBS N=9	<i>Igfbp2^{-/-}</i> PEG-HBD N=6
Bone volume/Total volume	0.314 ± 0.020	0.278 ± 0.010	0.305 ± 0.012 ^a
Trabecular number (1/mm)	6.15 ± 0.36	5.77 ± 0.11	5.70 ± 0.10
Trabecular thickness (mm)	0.052 ± 0.002	0.049 ± 0.001	0.054 ± 0.002 ^b
Trabecular spacing (mm)	0.155 ± 0.009	0.160 ± 0.004	0.161 ± 0.004

PEG-HBD: pegylated heparin-binding domain

Values are expressed as the mean ± SEM.

^a p=0.09 vs *Igfbp2^{-/-}* with PBS

^b p<0.05 vs *Igfbp2^{-/-}* with PBS

Table 3. Histomorphometric analysis of femur from male *Igfbp2*^{-/-} mice treated with PBS or PEG-HBD

	<i>Igfbp2</i> ^{-/-} PBS N=5	<i>Igfbp2</i> ^{-/-} PEG-HBD N=5
OS/BS (%)	2.38 ± 1.11	3.56 ± 0.44
ObS/BS (%)	11.5 ± 1.03	16.26 ± 1.42 ^a
Nob/BPm(/mm)	12.31 ± 0.52	16.3 ± 1.4 ^a
ES/BS (%)	17.11 ± 0.93	14.79 ± 01.58
OcS/BS (%)	11.02 ± 0.87	9.14 ± 0.90
Noc/BPm (/mm)	5.19 ± 0.37	4.37 ± 0.39
MAR (μm/day)	0.873 ± 0.0078	0.91 ± 0.0453
BFR/BSd (μm ³ /μm ² /day)	0.0796 ± 0.0164	0.080 ± 0.0191

PEG-HBD; pegylated heparin-binding domain, OS; osteoid surface, BS; bone surface, ObS; osteoblast surface, Nob; osteoblast number, BPm; bone perimeter, ES; erosion surface, OcS; osteoclast surface, Noc; osteoclast number, MAR; mineral apposition rate, BFR; bone formation rate

Values are expressed as the mean ± SEM

^a p<0.05 vs *Igfbp2*^{-/-} with PBS

Table 4. MicroCT analysis of femurs from female IGFBP2^{-/-} treated with PBS or PEG-HBD-peptide

	IGFBP2 ^{-/-} PBS N=10	IGFBP2 ^{-/-} PEG-HBD N=4
Midshaft		
Cortical thickness (mm)	0.176 ± 0.003	0.188 ± 0.003 ^a
Bone area (mm ²)	0.726 ± 0.018	0.791 ± 0.012
Total area (mm ²)	1.744 ± 0.038	1.830 ± 0.039 ^b
Bone area/Total area	0.417 ± 0.006	0.433 ± 0.008
Distal Femur		
Bone volume/Total volume	0.038 ± 0.001	0.049 ± 0.006 ^c
Trabecular number (1/mm)	2.99 ± 0.08	3.35 ± 0.12 ^c
Trabecular thickness (mm)	0.035 ± 0.001	0.036 ± 0.002
Trabecular spacing (mm)	0.338 ± 0.011	0.298 ± 0.011 ^c

PEG-HBD; pegylated heparin-binding domain

Values are expressed as the mean ± SEM.

a: p=0.06 vs IGFBP2^{-/-} with PBS

b: p=0.05 vs IGFBP2^{-/-} with PBS

c: p<0.05 vs IGFBP2^{-/-} with PBS

Figure 1

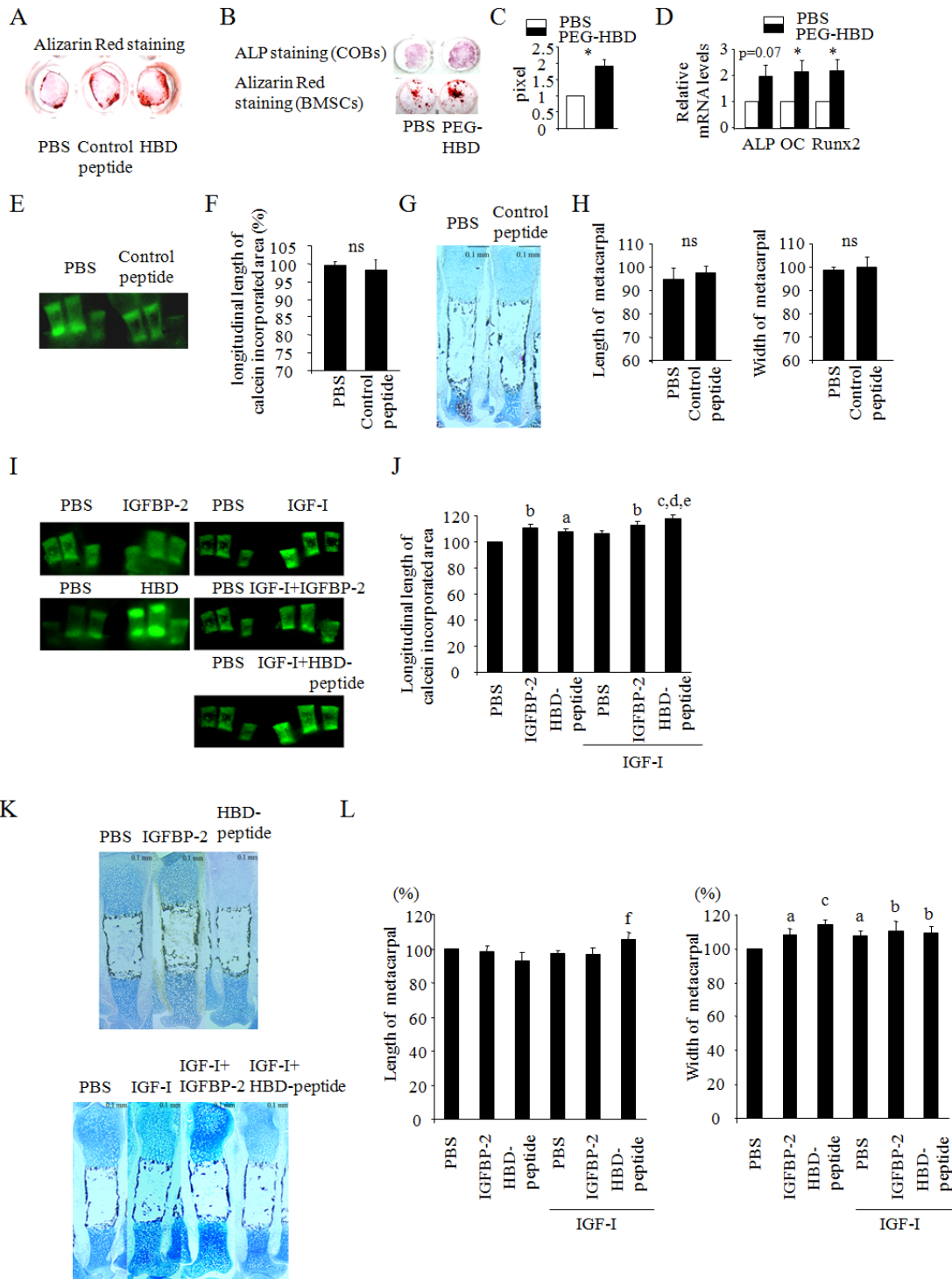


Figure 2

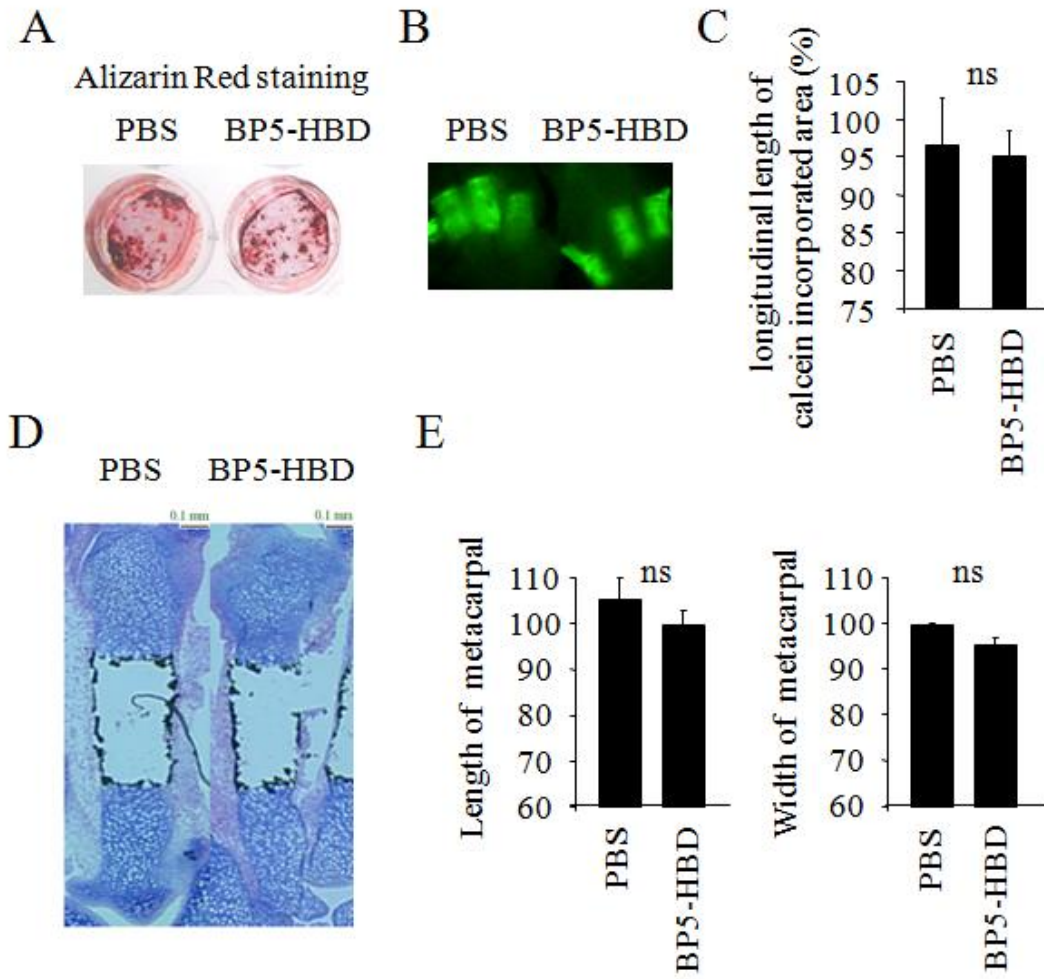


Figure 3

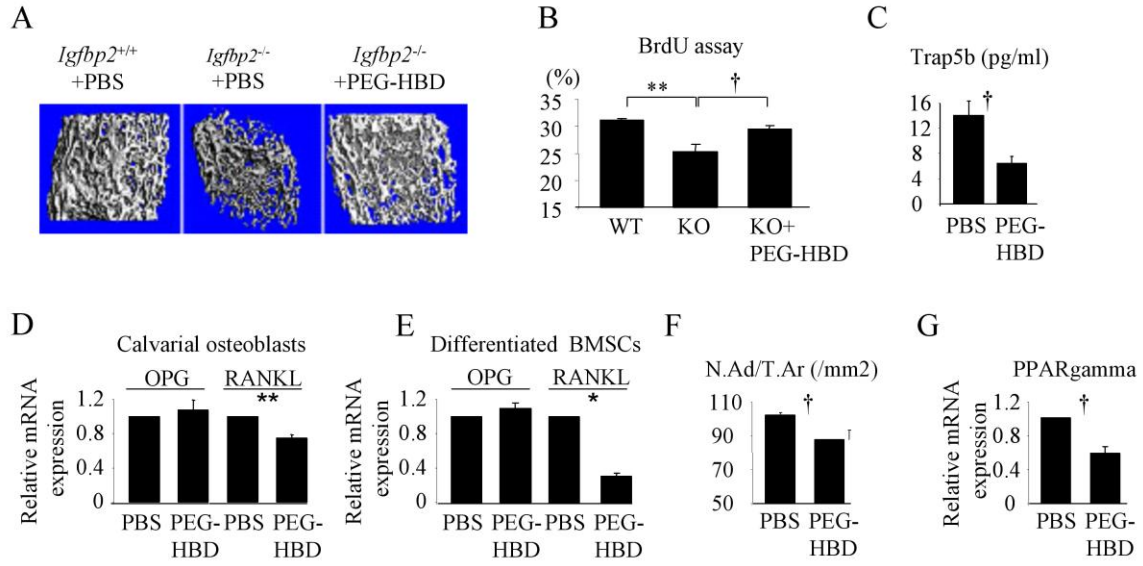


Figure 4

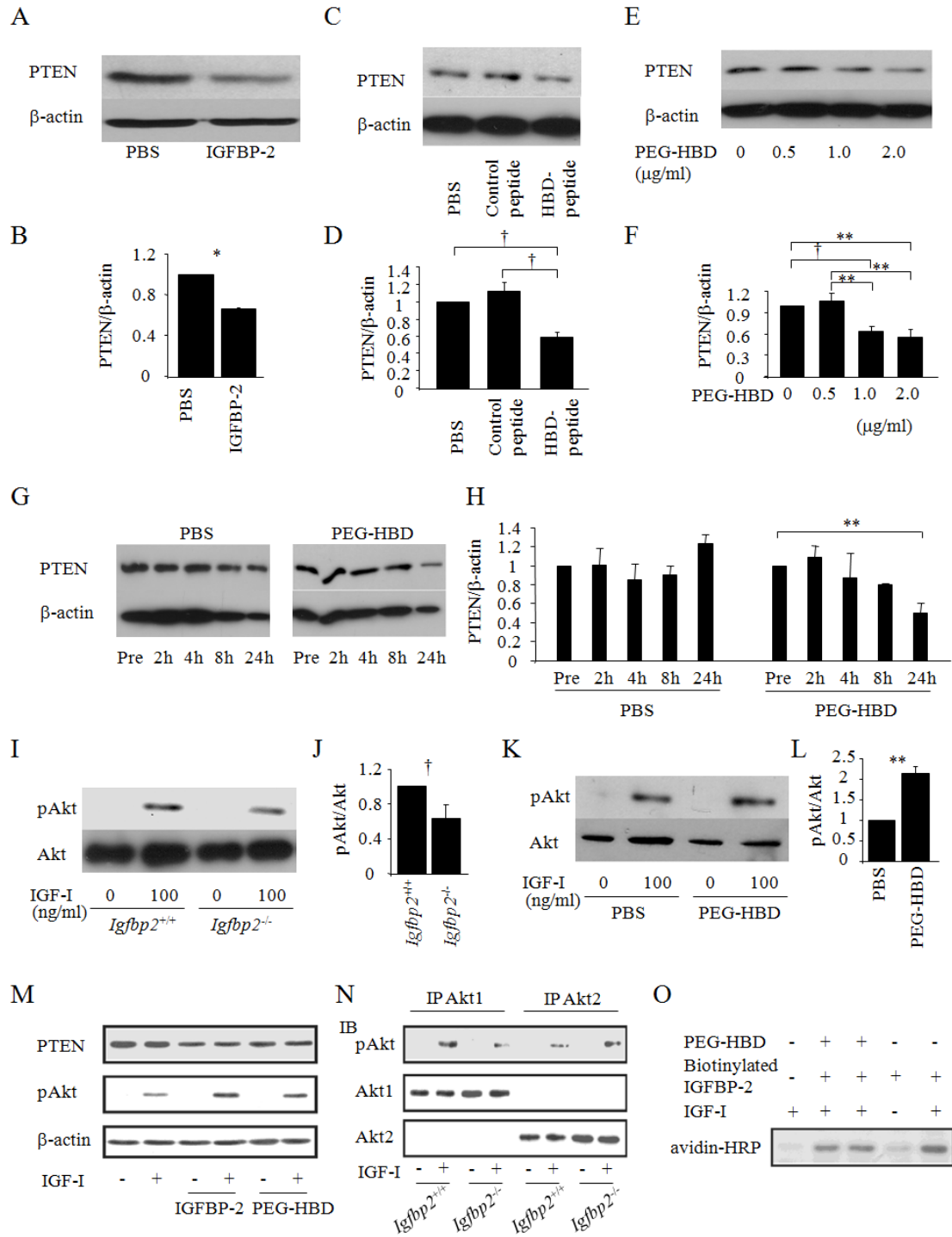


Figure 5

